Pergamon

Int. J. Solids Structures Vol. 35, Nos. 1–2, pp. 83–106, 1998

0020–7683/98 $19.00 + .00

PII: S0020–7683(97)00055–3

A DYNAMIC MODEL FOR LAMINATED PLATES WITH DELAMINATIONS

TODD O. WILLIAMS and FRANK L. ADDESSIO
Theoretical Division, Los Alamos National Laboratory, Los Alamos, NM, U.S.A.

(*Received* 17 *September* 1996; *in revised form* 9 *January* 1997)

Abstract—A generalized theory for laminated plates, including delamination, is developed. The laminate model is based on a generalized displacement formulation implemented at the layer level. The equations of motion for a layer, which are explicitly coupled with both the interfacial traction continuity and the interfacial displacement jump conditions between layers, are used to develop the governing equations for a laminated composite plate. The delamination behavior can be modeled using any general constitutive fracture law. The interfacial displacement jumps are expressed in an internally consistent fashion in terms of the fundamental unknown interfacial tractions. The current theory imposes no restrictions on the size, location, distribution, or direction of growth of the delaminations. Therefore, the theory can predict the initiation and growth of delaminations at any location as well as interactive effects between delaminations at different locations within the laminate.

The proposed theory is used to consider the dynamic response of laminated plates in cylindrical bending. First it is shown that the dynamic implementation agrees well with the exact predictions of a plate under static loading conditions. Static, cylindrical bending is considered to validate the numerical implementation. Next, different dynamic loading cases are considered. First, the required level of discretization through the thickness of the laminate necessary to accurately capture the wave propagation characteristics for monotonic tensile loading transverse to the plate is determined. Next, the influence of the delamination on the free vibration behavior of a plate is considered. It is shown that the presence of delaminations can result in significant deviations from the perfectly bonded free vibration behavior. Finally, the plate is subjected to dynamic loading conditions that demonstrate the influence of internal wave interactions on the overall behavior of the plate. © 1997 Elsevier Science Ltd.

1. INTRODUCTION

The use of laminated composite structures has many potential applications in a variety of engineering fields. Laminated structures are susceptible to delaminations between layers due to the low transverse strength at the interlaminar interfaces. Typically, delaminations in fibrous composites propagate along the fiber/matrix interfaces adjacent to the resin rich interlaminar region (Fig. 1). The presence of delaminations can cause significant degradation of the structural response characteristics. Therefore, analytical tools, which can accurately predict the behavior of delaminated structures as well as provide insight into methodologies for controlling delamination behavior, are valuable. The use of three-dimensional computational elements to predict the response of thin laminated structures to dynamic loads is inconvenient because of the number or aspect ratio of elements necessary to obtain numerical solutions. Therefore, an accurate plate or shell model for laminated structures is desirable.

Numerous applications of laminated structures require the support of dynamic or impact loads. Dynamic loading conditions can be induced by low velocity impacts (e.g. resulting from dropped tools), high velocity impacts (e.g. projectile impact), or simply as a result of the structural design and application. Structural deformation, tensile wave propagation transverse to the interfaces, or vibrational fatigue resulting from these loading conditions can result in the initiation of delamination damage. In some cases, such as low velocity impacts, there may be little visible damage at the structure surface even in the presence of significant damage within the composite. The presence of a delamination can result in redistributions of the internal stresses within the structure. These redistributions can result in the arrest of existing damage as well as the initiation and growth of delaminations in other regions within the structure. These issues imply that the extent of delamination damage is not known *a priori*. It cannot be assumed that the continued growth and direction

of growth of a delamination is self-similar. Both the initiation and growth of the damage must be accurately predicted to effectively model the behavior of a laminated structure in the presence of delaminations.

A plethora of work has been published concerning the behavior of delaminated structures. A partial review of some of the early work in this area was provided by Storakers (1989). More recent work has been considered in a review of Bolotin (1996). Typically, delamination behavior has been modeled using empirical delamination criteria (Ramkumar and Chen, 1983; Ramkumar and Thakar, 1987) or virtual crack extension methods (Barbero and Reddy, 1991; Chattopadhyay and Gu, 1994; Zheng and Sun, 1995; Galea *et al.*, 1995; Rinderknecht and Kröplin, 1995; Kutlu and Chang, 1995; Chen *et al.*, 1995; Hu and Hwu, 1995; Ju *et al.*, 1995; Lo *et al.*, 1993; Finn and Springer, 1993). Current crack extension methods have exhibited difficulties under mixed mode deformations (Sun and Qian, 1996; Narayan and Beuth, 1996). Less work has been pursued using interfacial constitutive laws to model delamination (Liu *et al.*, 1994). This work has been limited to the use of a simple linear model for the interfacial constitutive behavior. A linear delamination model can be used to study the initiation of delamination. However, this type of model can not be used for large interfacial displacement problems because in these situations the delamination growth is highly nonlinear (Needleman, 1987, 1990; Corigliano, 1993). Furthermore, this work has been restricted to elastic behavior due to the *a priori* implementation of the lamina elastic constitutive relations in satisfying the interfacial traction continuity conditions. History dependent behavior is a phenomena inherent to all composite materials.

A higher-order, discrete layer analysis, where each lamina is modeled individually, has the potential to correctly model delamination behavior because the individual interfaces are not smeared. Furthermore, a discrete layer theory can accurately predict local, nonlinear behavior such as plasticity and damage, which influences delamination. Recently, a formulation that is capable of incorporating any general nonlinear interfacial fracture model into a general plate theory was developed (Williams and Addessio, 1996). This approach was shown to provide excellent agreement with an exact solution under static loading conditions for delaminated plates. This approach can provide reasonable computational efficiency because of its two-dimensional nature while providing accurate predictions for the structural behavior.

The constitutive behavior for the fracture of interfaces, such as the interface between lamina within a composite structure, can be modeled by the following general relation (Aboudi, 1991; Needleman, 1987; 1990; Mcgee and Herakovich, 1992; Corigliano, 1993).

$$\Delta_i = f_i(\Delta_k, t_k) \tag{1}$$

where Δ_k is the jump in the displacement field across the interface and $t_k = \sigma_{ki}\, n_i$ is the interfacial traction vector. The unit normal to the interface and the stress field are n_i and σ_{ij}, respectively. In general, the constitutive relations for the jumps in the displacement field, $f_i(\Delta_k, t_k)$, are a nonlinear function of Δ_k and t_k. An accurate assessment of the interfacial traction is required to correctly predict delamination, using eqn (1). Changing the form of the delamination law should not require reformulating the entire plate theory.

In the current work, a formulation for a generalized theory of laminated plates in the presence of delaminations is presented (Williams and Addessio, 1996). The governing equations for the response of a single layer are developed and these equations are subsequently coupled through the explicit imposition of both interfacial traction continuity and the jump conditions for the interfacial displacements to develop the governing equations for a laminate. The basic variables of the resulting theory are the layer velocities and the interfacial tractions between layers. By treating the interfacial tractions as fundamental unknowns, an internally consistent evaluation of these effects is directly obtained from the formulation. The formulation is not restricted to the analysis of pre-existing delaminations and can predict the initiation and growth of delaminations. Additionally, the model is formulated in a sufficiently general fashion that any interfacial fracture model can be incorporated in an internally consistent fashion without reformulating the theory. Local

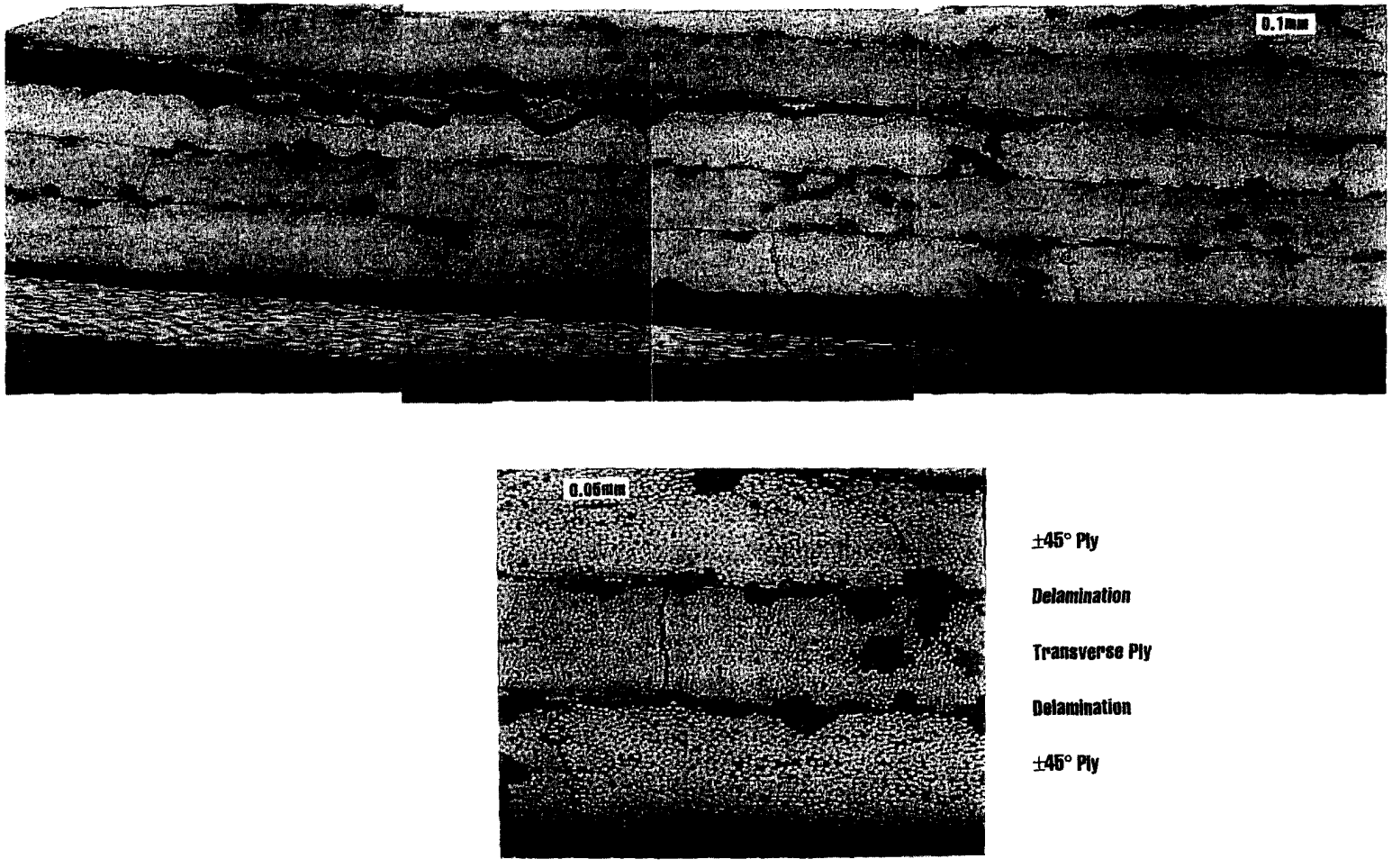

Fig. 1. Scanning electron micrograph of the tensile region of a four-point bend specimen illustrating delamination propagation along the fiber/matrix interfaces adjacent to the resin rich interlaminar region.

effects, such as the inelastic response of the lamina, can be modeled with any desired accuracy because no restrictions are imposed on the layer constitutive relations or the order of the approximation for the fields through the thickness of the layers. Finally, the resulting theory is completely general with respect to the thickness of the laminated structure.

The proposed formulation is used to consider the influence of delamination initiation and growth on the dynamic behavior of laminated plates. The numerical implementation of the theory is validated by comparison with an extension (Williams and Addessio, 1996) of the exact static solution (Pagano, 1967) for plates in cylindrical bending. This extension models the effects of delamination. Next, the appropriate level of discretization in the transverse direction that is necessary to accurately simulate the dynamic response in cylindrical bending is considered. The influence of delamination on the free vibration behavior of a cross-ply plate is considered. Finally, the influence of internal wave propagation and reflection on the overall response of a laminate in the presence of delaminations is investigated.

2. GENERAL FORMULATION

The following notational conventions are used throughout the formulation. Superscripts will denote the number (or order) of the approximation function. Subscripts denote tensorial quantities. Greek subscripts have a range of x and y. Roman subscripts have a range of x, y and z. Repeated superscripts and subscripts imply summation over the appropriate range. A comma denotes differentiation with respect to the spatial coordinates. A dot denotes differentiation with respect to time.

A single computational layer (k) is considered (Fig. 2). It is assumed that the velocity field (v_i) within this layer is approximated by

$$v_i(x, y, z, t) = V_i^j(x, y, t)\phi^j(z) \tag{2}$$

where $j = 1, 2, \ldots, N$. N is the order of the polynomial expansion for the computational layer. This approximation has been used to model perfectly bonded laminates (Reddy, 1987). The $\phi^j(z)$ are specified functions of the transverse coordinate z and the $V_i^j(x, y, t)$ are the velocity coefficients in the i-direction associated with the j-polynomial. Equation 2 admits any order of approximation because no restriction is placed on the order or functional form of the $\phi^j(z)$. The corresponding rate of deformation field within the layer is given by

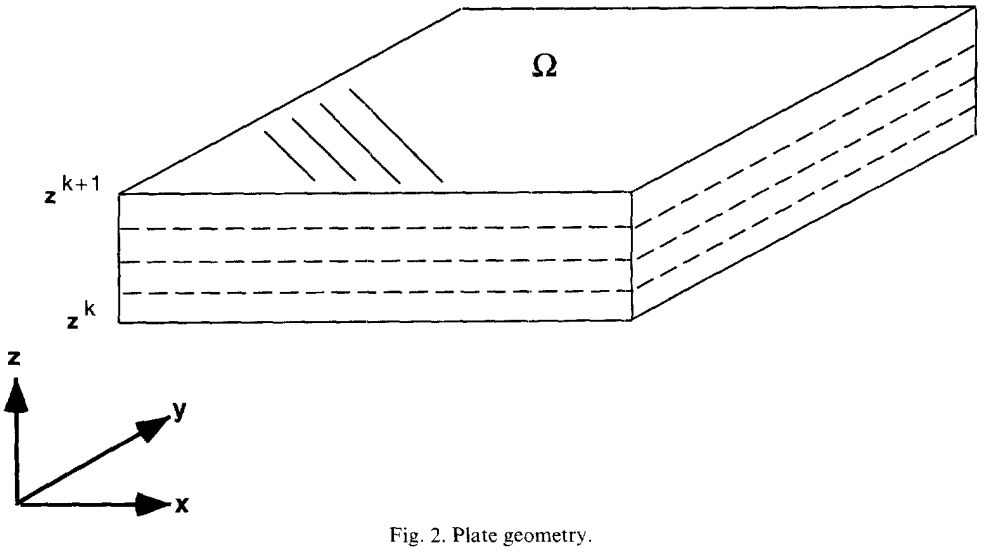

Fig. 2. Plate geometry.

$$D_{ij} = \tfrac{1}{2}(v_{i,j} + v_{j,i}) \tag{3}$$

where v_i is provided by eqn 2. The formulation of the governing equations for the layer are obtained from the application of the principle of virtual work (Washizu, 1968; Reddy, 1984).

$$\int_0^t \left(\int_V \sigma_{ij} \delta D_{ij} \, \mathrm{d}V - \int_S t_i^* \delta v_i \, \mathrm{d}S - \int_V f_i \delta v_i \, \mathrm{d}V - \int_V \rho \dot{v}_i \delta v_i \, \mathrm{d}V \right) \mathrm{d}t = 0 \tag{4}$$

where σ_{ij} denote the Cauchy stresses, t_i^* denote the surface tractions, f_i are the body forces, and ρ is the density. In the above equation, the appropriate volume to be used is that of the layer given by $V = h_k \cdot \Omega$ (Fig. 2). The thickness of the kth layer is given by $h_k = z^{k+1} - z^k$, where z^{k+1} and z^k are the coordinates of the top and bottom of the layer, respectively. Ω is an arbitrary area corresponding to the midplane of the layer. S is the outer surface area of the volume V.

Substituting eqns 2 and 3 into eqn 4 and integrating through the thickness (z) to obtain an equivalent two-dimensional theory gives

$$\int_0^t \left(\oint_{\partial\Omega} (T_i^j - N_{i\alpha}^j n_\alpha) \delta V_i^j \, \mathrm{d}s + \int_\Omega (\tau_i^j + N_{i\alpha,\alpha}^j - R_i^j + F_i^j - I^{mj} \dot{V}_i^m) \delta V_i^j \, \mathrm{d}\Omega \right) \mathrm{d}t = 0$$

where $\partial\Omega$ denotes the boundary of Ω and $\mathrm{d}s$ is the associated differential arc length. Consequently, the appropriate equations of motion for the layer are

$$\tau_i^j + N_{i\alpha,\alpha}^j - R_i^j + F_i^j = I^{mj} \dot{V}_i^m \tag{5}$$

where $m, j = 1, 2, \ldots, N$. The corresponding inplane boundary conditions are

$$\begin{aligned} V_i^j &= V_i^{j*} \quad \text{on } \partial\Omega_{\mathrm{I}} \\ N_{i\alpha}^j n_\alpha &= T_i^j \quad \text{on } \partial\Omega_{\mathrm{II}} \end{aligned} \tag{6}$$

where $\partial\Omega = \partial\Omega_{\mathrm{I}} + \partial\Omega_{\mathrm{II}}$ and V_i^{j*} are specified boundary velocities. The n_α are the unit normals along the boundary $\partial\Omega$. The first set of conditions in eqn 6 represent the essential boundary conditions. The second set of conditions represent the natural boundary conditions. In developing the above results the following definitions where used

$$N_{rs}^j = \int_{z^k}^{z^{k+1}} \sigma_{rs} \phi^j \, \mathrm{d}z \tag{7}$$

$$R_i^j = \int_{z^k}^{z^{k+1}} \sigma_{rz} \phi_{,z}^j \, \mathrm{d}z \tag{8}$$

$$\tau_i^j = \sigma_{iz} \phi^j \Big|_{z^k}^{z^{k+1}} \tag{9}$$

$$T_i^j = \int_{z^k}^{z^{k+1}} t_i^* \phi^j \, \mathrm{d}z \tag{10}$$

$$F_i^j = \int_{z^k}^{z^{k+1}} f_i \phi^j \, dz \tag{11}$$

and

$$I^{jm} = \int_{z^k}^{z^{k+1}} \rho \phi^j \phi^m \, dz. \tag{12}$$

The terms τ_i^j are related to the interfacial tractions. The $N_{i\alpha}^j$ and R_i^j are force resultants. The F_i^j correspond to body force effects. The I^{jm} represent the inertial effects.

It is emphasized that eqns 5 and 6 represent the equations of motion and appropriate boundary conditions, respectively, governing the response of a *single* computational layer. A computational layer may be thinner than a typical lamina in a structure, of equal thickness to a lamina, or it may be composed of several lamina. It is emphasized that these equations were developed independently of any structural considerations related to the laminated structure.

Explicit satisfaction of both the continuity of the interfacial tractions and the jump conditions on the interfacial displacements are utilized to couple the equations governing the behavior of different layers to obtain the governing equations for the laminate. These interfacial conditions are given by

$$v_i^{k+1} - v_i^k = \dot{\Delta}_i^k \tag{13}$$

and

$$\sigma_{iz}^k = \sigma_{iz}^{k-1} \tag{14}$$

where $\dot{\Delta}_i^k$ represents the jump in the ith velocity component across the interface between the kth$+1$ and kth layers. The constitutive relation for $\dot{\Delta}_i^k$ is provided by an interfacial constitutive model (eqn 1).

The interfacial constraints (eqns 13 and 14) are easily imposed if it is assumed that the $\phi^i(z)$ are Lagrange polynomials of order j. These polynomials have the following property

$$\phi^i(z_j) = \delta_{ij} \tag{15}$$

where δ_{ij} is the Kronecker delta. This property makes the satisfaction of the interfacial constraints particularly simple. It is noted that the use of Lagrange polynomials is based on convenience only. Substituting eqn 15 into eqn 9 gives

$$\begin{aligned} (\tau_i^1)^k &= (t_i^1)^k = -\sigma_{iz}^k|_{z^k} \\ (\tau_i^N)^k &= (\tau_i^N)^k = \sigma_{iz}^k|_{z^{k+1}} \\ (\tau_i^j)^k &= 0 \quad \text{for } j = 2, 3, \ldots, N-1. \end{aligned} \tag{16}$$

Therefore, the interfacial traction continuity conditions, eqn 14, are satisfied by

$$(\tau_i^j)^k + (\tau_i^j)^{k+1} = 0. \tag{17}$$

The jump conditions for the velocities (eqn 13) at the kth interface are satisfied by

$$(V_i^1)^{k+1} - (V_i^N)^k = \dot{\Delta}_i^k = \dot{f}_i(\Delta_m^k, t_m^k) \tag{18}$$

for an Nth order Lagrange polynomial in z. Using eqn 16, the functional form for the velocity jump (eqn 1) can be rewritten as

$$\dot{\Delta}_i^k = \dot{f}_i(\Delta_m^k, \tau_m^k). \tag{19}$$

Equation 19 is completely general but now the velocity jumps are expressed in a direct and consistent fashion as a function of the fundamental unknowns in the theory. Additionally, use of an interfacial function of the type given in eqn 19 can easily incorporate the constraint that the layers cannot interpenetrate.

The equations of motion (eqn 5) subject to the interfacial constraints (eqns 17–19) in conjunction with the layer boundary conditions (eqn 6) form the system of equations governing the behavior of the laminated structure. The fundamental variables in the theory are the layer velocity coefficients (V_i^j) and the interfacial tractions (τ_i^j).

The current formulation has several unique features that differentiate it from existing theories. Any general interfacial constitutive law can be used to determine the behavior of the structure in the presence of delaminations in a internally consistent fashion. Changing the interfacial fracture behavior does not require a reformulation of the current theory. This formulation is not restricted to modeling preexisting delaminations and can predict the initiation and growth of delaminations anywhere within the structure. The growth of these delaminations is not in any way restricted to a given location or direction. The current approach can be directly applied to model the inelastic deformation of composite structures. Furthermore, no restrictive assumptions regarding the constitutive response of the layers have been imposed.

3. NUMERICAL IMPLEMENTATION OF THE DYNAMIC THEORY

This section discusses two types of formulations for the implementation of the dynamic theory. The first section discusses a solution methodology based on the use of a Fourier series approach to model the spatial derivatives in the cylindrical bending problem. The second section discusses the implementation of a general, finite element formulation for the theory.

Both numerical approaches utilize explicit time integration schemes to obtain the solution. A forward difference is used to approximate the temporal derivative

$$\dot{v} = \frac{v - v_o}{\Delta t} \tag{20}$$

where v is the current velocity at a point in the plate and v_o is the value of the velocity at the beginning of the time step ($t = t_o$). Because an explicit integration scheme is used, the spatial gradients used to advance the solution are evaluated using the velocity field at the time t_o. The computation techniques are initiated by determining the time-step size (Δt), which provides a stable solution.

3.1. *Harmonic solution formulation*

In the harmonic solution (HS) for an infinite strip, the spatial dependence is satisfied exactly using Fourier series to describe the velocities. The velocity field, which satisfies the boundary conditions, is given by

$$\begin{aligned} v_x &= V_z^{jn}\phi^j(z)\cos p^n x \\ v_y &= 0 \\ v_z &= V_z^{jn}\phi^j(z)\sin p^n x \end{aligned} \tag{21}$$

where $p^n = n\pi/L$ and n is the harmonic number. Substituting the above velocity field and the finite difference approximation (eqn 20) into the governing differential equations for the plate theory (eqn 5) provides a system of equations for a layer (for each harmonic) of the form

$$I^{mj}V_i^m - \tau_i^j \Delta t = I^{mj}V_i^m(t_o) - K_{ik}U_k^j \Delta t \tag{22}$$

where U_k^j are the displacement coefficients at time t_o, and K_{ik} is a function of the geometric and material properties of the layer as well as the harmonic number. It is emphasized that the vector τ_i is evaluated at the current time (t) while the right-hand side of eqn 22 is evaluated at time t_o. This system in conjunction with the interfacial conditions (eqns 17–19) provides the necessary equations for the determination of the velocities (V_i^{jn}) and interfacial stresses (τ_i^{jn}).

3.2. *Finite element formulation*

A general, finite-element (FE) formulation of the plate theory was developed to pursue the dynamic response of composite structures. A finite element implementation is obtained using the layer equations of motion (eqn 5). For convenience, the stresses are approximated as

$$\sigma_{ij} = \Sigma_{ij}^{\ell m}(t)\psi^{\ell}(x, y)\phi^m(z) \tag{23}$$

where

$$\Sigma_{ij}^{\ell m}(t)$$

are the values of the stresses at the nodal locations and $\phi^m(z)$ are the transverse shape functions. A quadratic distribution was used in the transverse direction. A bilinear approximation was used for the inplane shape functions $\psi^{\ell}(x, y)$. The inplane stress gradients necessary to compute the terms $N^j_{iz,\alpha}$ (eqn 5 and 7) were obtained using the Mean Value Theorem. For example, for an arbitrary interior node

$$\left\langle \frac{\partial \sigma_{ix}}{\partial x} \right\rangle^m = \left(\int \Psi^m \frac{\partial \Psi^n}{\partial x} \, d\Omega \right) \sigma_{iz}^n \Big/ \int \Psi^m \, d\Omega \tag{24}$$

where the area integrals include the four inplane elements surrounding the mth node. There is no summation on the subscript m in eqn 24. A similar expression was used to obtain the partial derivatives with respect to the y-direction. Similar to the harmonic solution, an explicit formulation was used to advance the equations in time. That is, the left-hand side of eqn 5 is assumed to be known, using values from the previous time step. The equations of motion, coupled with continuity of interfacial tractions and the interfacial constitutive equation, provide a system of equations for the through plane velocities (V_i^j) and interfacial stresses (τ_i^j) for each position (x_m, y_n) on the plate. The formulation provides for doubly defined velocities on the layer interfaces. To reduce the number of equations, the interfacial constitutive relations were used to eliminate the velocities at the bottom of each computational layer. For each time step of the finite-element formulation, the solution procedure is advanced by applying the following steps:

(1) the stress gradients (eqn 24) are calculated
(2) the governing equations (eqns 5, 6 and 17–19) are solved for the nodal velocities and interfacial tractions at each position (x_m, y_n)
(3) the displacements are updated for graphical output
(4) the velocity gradients, which are used to determine the rate of deformation tensor (eqn 3), are updated

(5) the constitutive model for the lamina is used to update the nodal stresses.

Steps (1) through (5) are invoked until the end of the problem (t_{end}) is reached. Similar to the stress gradients, the velocity gradients necessary to compute the rate of deformation tensor (eqn 3) for step 4 are computed using the Mean Value Theorem. That is, $\partial v_i/\partial x_j$ are obtained using a relation similar to eqn 24 with the surface (Ω) integrals replaced by volume integrals and using a tri-linear shape function $\psi^m(x, y, z)$.

The FE implementation of the theory is limited to small deflections because it is assumed that the model parameters in the current configuration can be obtained at the locations of the undeformed configuration. It is felt that this is a reasonable assumption for graphite reinforce composites, which fracture at relatively small strains. Furthermore, the sample problem considered are only carried out to small strains. The generalization of the FE implementation for large deformations would simply require updating the model parameters on the current configuration.

4. RESULTS

The proposed plate theory is used to consider the influence of delaminations on the dynamic response of composite cross-ply plates subjected to cylindrical bending. The cylindrical bending problem is based on the analysis of a simply supported infinite strip. The geometry of the cylindrical bending problem is provided in Fig. 3. The perfectly bonded solution is provided by Pagano (1969). Further details of the cylindrical bending problem for delaminated plates are given by Williams and Addessio (1996). The sample problems have been chosen for convenience. The simple geometries used in the simulations have potential applications in experimental investigations for the characterization of composite interfacial properties. To model more complex composite structures, it is necessary to include a larger number of laminates in the simulations. This can be accomplished using one of two approaches. More computational layers can be included in the simulations or an homogenization theory can be added to the theory, allowing each computational layer to model more than one laminae.

The following conditions are assumed to apply to all of the results. The plate aspect ratio, (S) is assumed to be 5. Thus, the plate can be considered to be thick. Because of the relatively small aspect ratio, shearing deformations in the transverse direction are important for this case. The effective material properties of the lamina are given by

$$E_L/E_T = 25 \quad G_{LT}/E_T = 0.5 \quad \nu_{LT} = \nu_{TT} = 0.25 \quad \rho = 1.56\ \text{g/cm}^3 \tag{26}$$

where the subscripts T and L represent the transverse and longitudinal directions in the lamina principle coordinate system, respectively. These material properties represent the elastic behavior of a unidirectional graphite fiber-reinforced, epoxy matrix (Gr/Ep) com-

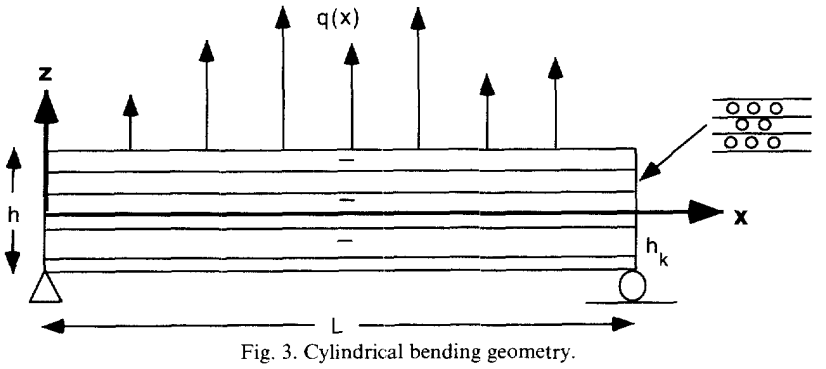

Fig. 3. Cylindrical bending geometry.

posite system. For this study, the delamination constitutive model is assumed to be linear (Aboudi, 1991) and is given by

$$\Delta_i = R\tau_{iz} \tag{27}$$

where the interfacial stiffness (R) may differ for the normal (R_n) and shear (R_s) responses, respectively. The laminates are assumed to be perfectly bonded initially, for the simulations considered.

The nondimensional parameters originally proposed by Pagano (1969) are used in presenting the results

$$\sigma_{xx}^* = \frac{\sigma_{xx}}{q} \quad \sigma_{zz}^* = \frac{\sigma_{zz}}{q} \quad \sigma_{xz}^* = \frac{\sigma_{xz}}{q}$$

$$u_x^* = \frac{E_T u_x}{hq} \quad u_z^* = \frac{100 E_T h^3 u_z}{L^4 q}$$

$$S = \frac{L}{h} \quad z^* = \frac{z}{h} \quad x^* = \frac{x}{L} \quad R^* = \frac{RE_T}{h}. \tag{28}$$

In eqn 28, h is the total laminate thickness and L is the plate length. For the current study, the loading is represented by the first term in a half sine series (q). All approximate plate theory results presented are generated using a second order theory [i.e. a quadratic polynomial is used for $\phi^j(z)$].

The first case considered is the quasi-static deformation of a cross-ply (0°/90°) plate. This case is intended to provide a limiting validation of the solution methodology. The fibers in the bottom lamina (90°) are aligned in the y-direction. The fibers are aligned in the x-direction (0°) in the top lamina. Each lamina is composed of two computational layers. Values of $R_n^* = 50$ and $R_s^* = 25$ were used for the normal and shear interfacial stiffnesses, respectively. The through the thickness distributions of the axial displacement (u_x^*) for the exact (Williams and Addessio, 1996) and HS at the edge of the plate ($x^* = 0.0$) are presented in Fig. 4. It may be seen that the correlation between the HS and the exact result is excellent. The displacement jump due to delamination is accurately predicted by the approximate theory with only negligible differences between the two results. The deviations between the exact and HS results are less than 0.4% of the overall change in the displacement through the thickness at all locations. Equally good agreement is obtained for the distributions of the transverse displacement (u_z^*) and axial stress (σ_{xx}^*) through the thickness. These comparisons are not provided in this paper.

The second case examines the influence of the different levels of discretization through the thickness on the behavior of a plate loaded dynamically under a transverse monotonic tensile load. Both the HS and FE formulations are considered. For this simulation, a linearly increasing load is applied for 5 μs. The laminate consists of a 0°/90° lay-up with the 90° lamina on the bottom of the plate. The results obtained from the harmonic solutions are considered first. To generate these results the individual lamina were discretized using 1, 2 and 10 computational layers per lamina. Also included in the figures (Figs 5–8) for this case are the perfectly bonded results as predicted using 2 layers per lamina. The values for the interfacial stiffness parameters (R_n^* and R_s^*) are arbitrarily assumed to be 1.0.

The structural response, as represented by the normalized transverse deflections at the interface between lamina of the plate as a function of time, is provided in Fig. 5. Examination of this figure indicates that, in general, using two or more computational layers per lamina results in very little deviation in the predictions. The transverse deflections above and below the interface ($z^* = 0$) exhibit increasingly greater differences as the loading increases for all levels of discretization. At a time of 5 μs the relative difference in the magnitudes is about 25% (for the converged response). It is important to note that the current approach correctly precludes the interpenetration of adjacent lamina. Comparison of the perfectly

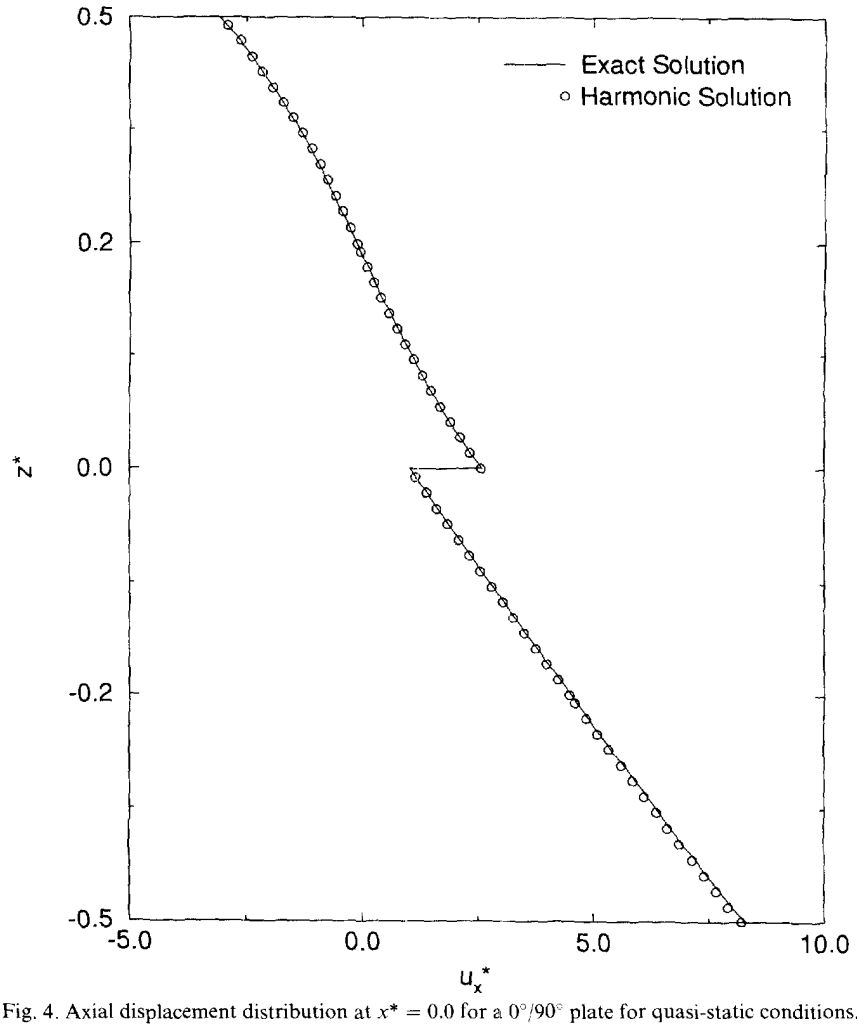

Fig. 4. Axial displacement distribution at $x^* = 0.0$ for a 0°/90° plate for quasi-static conditions.

bonded and delaminated responses shows that the perfectly bonded response falls between the transverse deflections at the top and bottom of the interface in the delaminated cases. As expected, the presence of a delamination delays the onset of significant transverse deflections at the bottom surface as compared to the perfectly bonded case. Using two layers per lamina results in only minor differences (about 1.5% of the magnitude at 5 μs) between 1.75 and 2.5 μs compared to the results using 10 layers per lamina. After 2.5 μs, the predictions obtained using two layers per lamina converge to those obtained using more through the thickness refinement. It is useful to consider the behavior predicted using one layer per lamina because this case results in the smallest computational times. Examination of these figures does indicate that the use of a single layer per lamina results in some deviations in the predictions compared to the results obtained using higher levels of discretization. At a time of 2.2 μs the use of one layer per lamina causes the transverse deflection to drop below zero reaching a value of about -0.006. When higher discretizations are used, the deflection remains essentially zero. However, this difference only represents about 2.2% of the total deflection at a time of 5 μs. As the loading increases, the predictions using one layer per lamina converge to the results predicted using finer levels of discretization. After about 4 μs some deviation again is observed, with the results predicted by the single layer per lamina case being larger than the other cases by about 3%. The above results demonstrate that the proposed model can predict the structural response using only one computational layer per lamina.

The distributions of the axial displacement (u_x^*) through the thickness of the plate at $x^* = 0$ for the second simulation is given in Fig. 6. All levels of discretization predict the

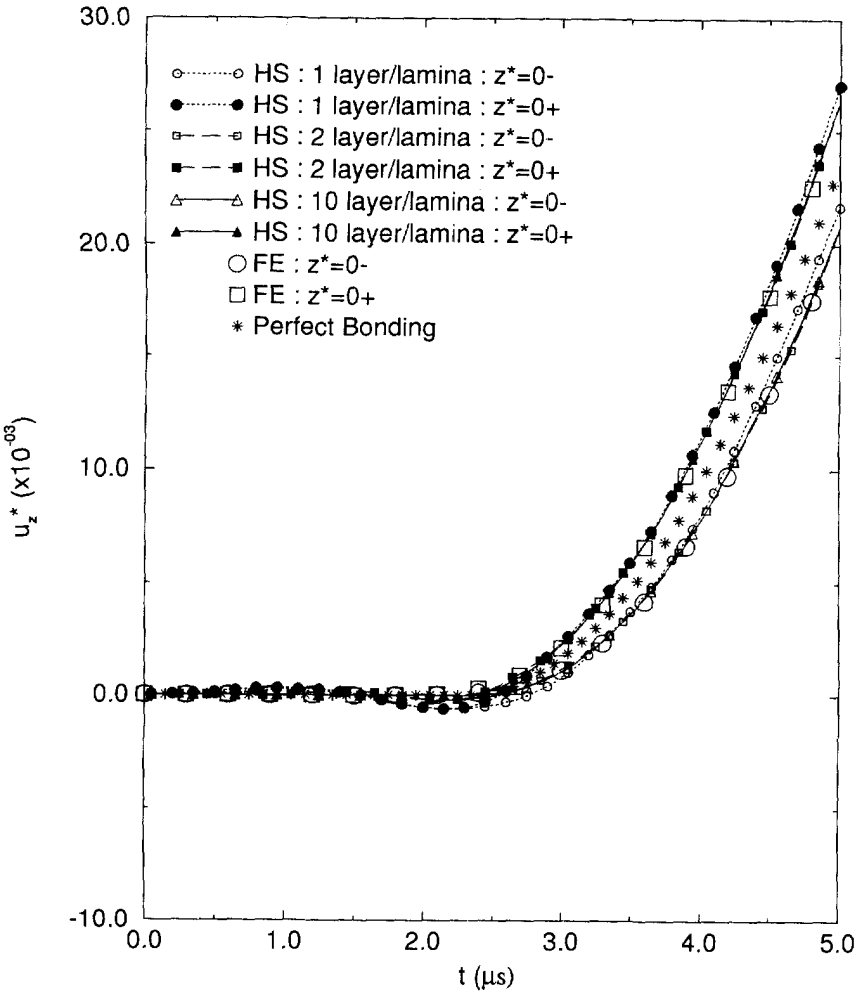

Fig. 5. Transverse deflections at $x^* = 0.5$ for a 0°/90° plate for dynamic conditions for the mid-plane response.

same general trends in the variation of u_x^* through the thickness. The general predicted behavior exhibits a contraction in u_x^* at the top surface. This behavior is consistent with the simply supported boundary conditions, which allow lateral motion and rotation of the ends. Much of the dynamic response is restricted to the top lamina for this loading situation. The axial displacements at the top and bottom of the upper lamina represent the extremes in the distribution. The bottom lamina exhibits a total change in the displacements that is only about one third of the displacement for the top lamina at 5 μs. The bottom surface has not been significantly influenced by the applied loading and the displacement is nearly zero. The displacement jump resulting from delamination represents about 10% of the change in the extremes of the distribution. Therefore, delamination can be considered to be a significant deformation effect for this case. Comparing the perfectly bonded and delaminated predictions shows that the perfectly bonded case exhibits trends, which are similar to the delaminated results. As the distance from the interface increases, the two sets of results converge. At the interface, the perfectly bonded predictions fall between the delaminated results, as expected. The perfectly bonded results do not bisect the displacement jump at the interface in the delaminated case but fall closer to the displacement value observed in the lower lamina. Using two or more layers per lamina in the analysis results in essentially converged predictions. Use of only one layer per lamina results in deviations in the top layer near the interface and at the outer surface of the bottom lamina. The magnitude of the displacement jumps predicted by all levels of discretization exhibit negligible differences. This trend is due to the fact that the interfacial tractions are treated as

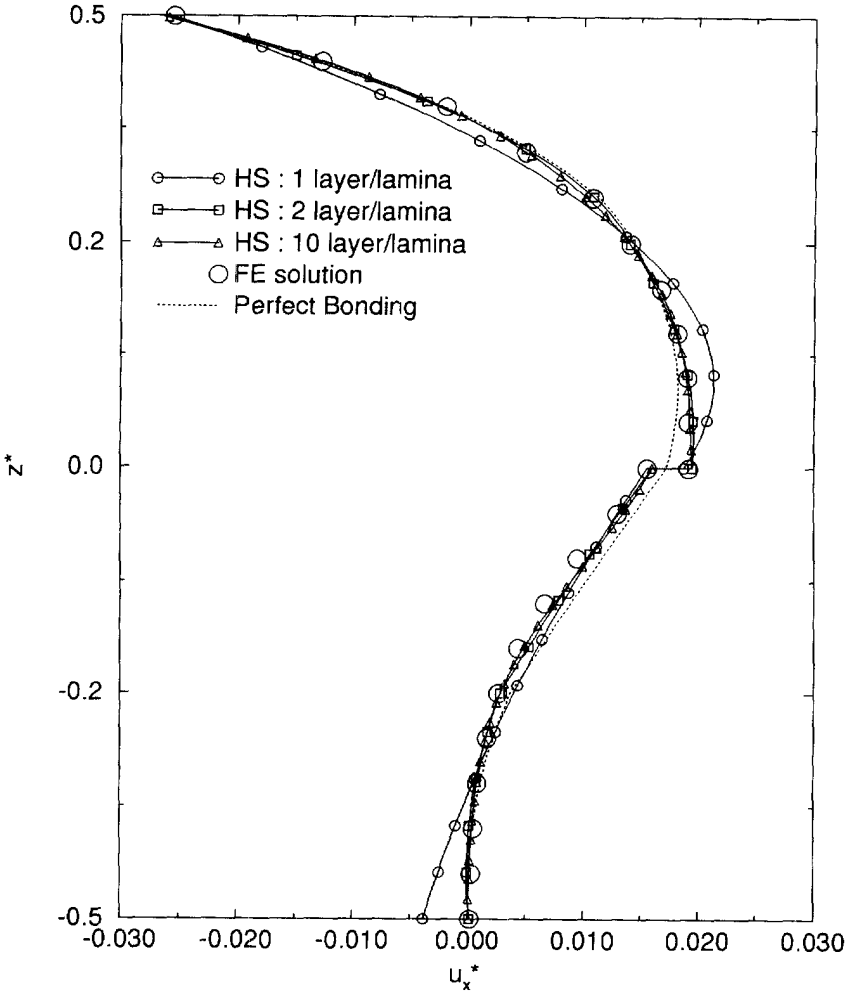

Fig. 6. Axial displacement distribution at $x^* = 0.0$ for $0°/90°$ plate for dynamic conditions at $t = 5$ μs.

fundamental variables and are relatively independent of the level of discretization used in the analysis. The level of discretization used, however, does cause a shift in the values of u_x^* above and below the interface. When 1 layer per lamina is used, the values of u_x^* are shifted to slightly smaller values at these locations as compared to the higher levels of discretization.

The transverse deflection (u_z^*) distribution through the thickness of the laminate at the midplane ($x^* = 0.5$) is presented in Fig. 7 at 5 μs. The agreement in the predictions obtained using all degrees of discretization is good with only small deviations. A maximum deviation of about 1.5% is observed in the case where the behavior of the plate is modeled using one layer per lamina. As expected, the predictions indicate that the current dynamic loading results in most of the response occurring in the upper lamina. The maximum deflection in the lower lamina, which occurs at the interface, represents only about 25% of the total maximum deflection. The displacement jump represents an additional 6.8% of the total deflection. As observed in the axial displacement distributions, the perfect bonding case falls within the jump observed for the delaminated behavior. The magnitude of the deflection in the perfect bonding case is closest to the response in the lower lamina at the interface for the delaminated case. As the distance increases away from the interface, the perfectly bonded and the delaminated distributions converge.

The axial stress (σ_{xx}^*) distribution through the thickness at $x^* = 0.5$ is presented in Fig. 8 at 5 μs. As in the previous results all levels of discretization predict the same general distributions. Much of the dynamic loading is supported by the top lamina as indicated by

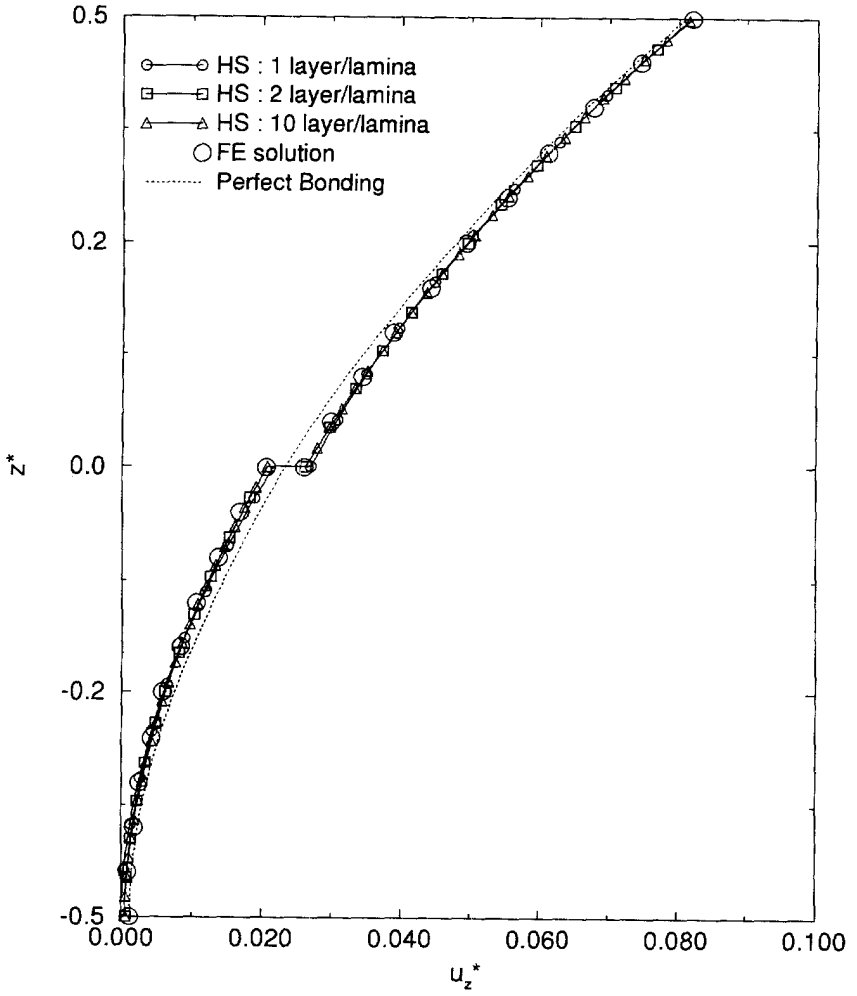

Fig. 7. Transverse deflections at $x^* = 0.5$ for a $0°/90°$ plate for dynamic conditions at $t = 5\ \mu s$.

the fact that the top lamina supports both extremes in the stress. This is consistent with the fact that the dynamic loading is applied at the top surface and that the top lamina is significantly stiffer in the x direction than the bottom lamina. All levels of discretization except for the case of one layer per lamina exhibit negligible deviations. In the case where the behavior of the laminate is modeled using one layer per lamina, appreciable deviations can be observed in the top lamina in the region near the interface. However, at the interface, all levels of discretization predict the same magnitude for the jump in the distribution. Comparison with the perfectly bonded case indicates that the influence of the delamination occurs primarily in the regions nearest to the interface. In the case of the bottom (90°) lamina this influence is small. However, in the top (0°) lamina the presence of the delamination increases the magnitude of the compressive stress at the interface by 16%.

The FE predictions also are provided in Figs 5–8 for comparison with the harmonic formulation. It is noted that the FE predictions exhibit convergence behavior that is equivalent to the trends observed in the predictions obtained from the harmonic formulation. The gross structural behavior as given by the transverse deflection versus time predicted by the FE solution exhibits negligible differences with the corresponding behavior predicted by the HS (Fig. 5). Comparison of the HS and FE model predictions for the distribution of u_x^* (Fig. 6) shows that the two formulations agree closely. Relatively minor variations of about 2% in the distribution can be observed in the region around the interface. The differences in the displacement jumps between the FE and HS is about 8% of the magnitude of the displacement jump. Good agreement is obtained for the FE and harmonic predictions for the distribution of u_z^* as well as the jump in the transverse

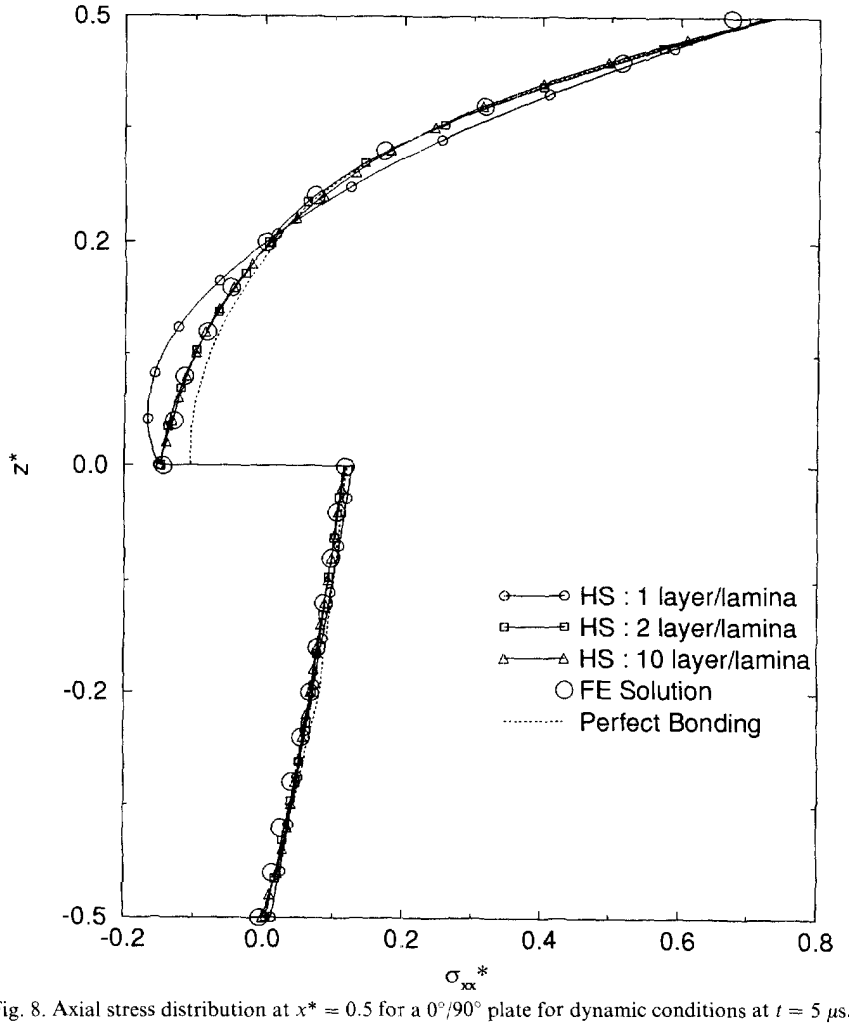

Fig. 8. Axial stress distribution at $x^* = 0.5$ for a 0°/90° plate for dynamic conditions at $t = 5$ μs.

displacement (Fig. 7). The axial stress distributions (Fig. 8) predicted by the two approaches also are in good agreement. The largest variations between the predictions of the two solutions occur in the 0° layer in the region near the top surface. These deviations can be primarily attributed to the small variations in the axial displacement in the regions near the surface.

Next, an impulsive tensile loading followed by free vibration is considered. The impulsive load reaches a maximum at 1 μs. The load is subsequently reduced to zero over another microsecond. The plate (0°/90°) then is allowed to vibrate freely for the next 1000 μs. The normalizing load in this case is the maximum applied load during the initial impulse. The interfacial stiffness parameters (R_n^* and R_s^*) are assumed to be 10 for this case. The time dependent transverse deflection (u_z^*) at the interface of the laminate for both the perfectly bonded and delaminated cases is presented in Fig. 9. The perfectly bonded case exhibits sinusoidal behavior with constant periods of oscillation and peaks. The period in the perfectly bonded case is about 155 μs. The peak value is nearly 0.2. The behavior in the presence of the delamination is significantly different. The period of oscillation is again constant and has a similar magnitude as the perfectly bonded case. Unlike the perfectly bonded case, the presence of the delamination results in divergent deflections at the top and bottom surfaces of the interface. The magnitude of the deflection at the top surface continues to increase while the magnitude becomes more negative at the bottom surface as time increases. The rate at which the magnitude in the deflection is changing is greater for the bottom surface than the top surface. This difference in the rates of growth of these two

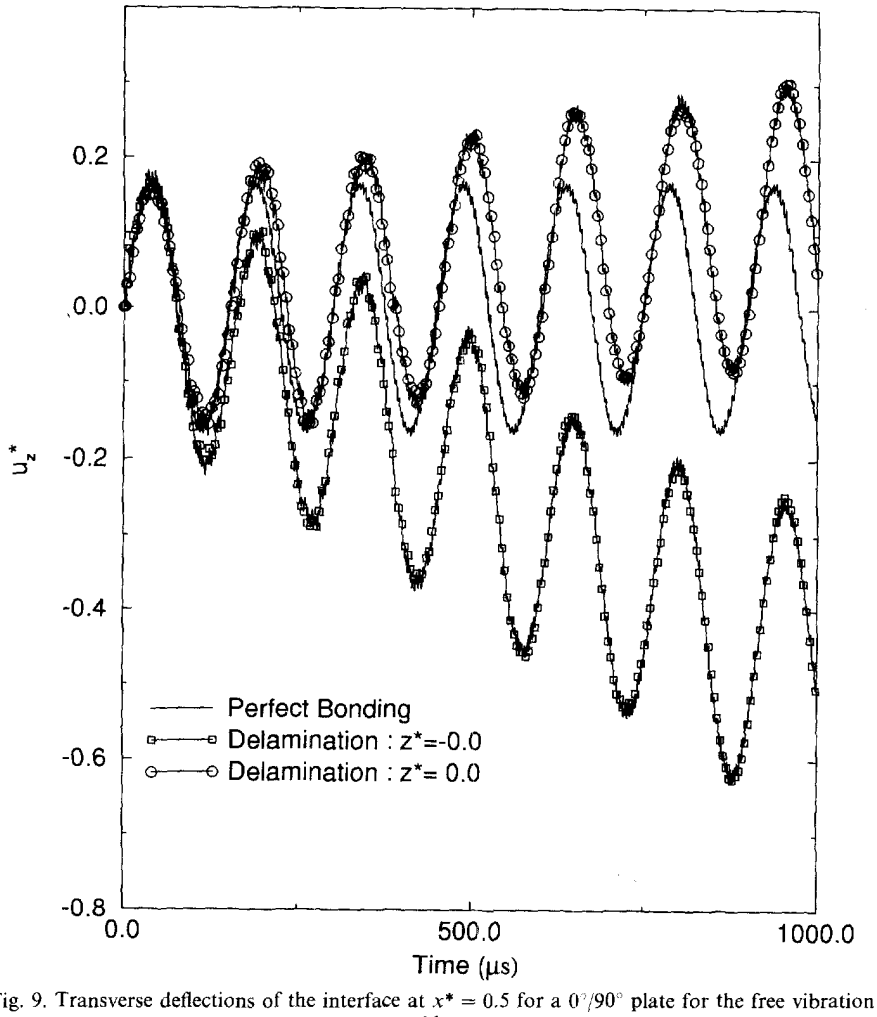

Fig. 9. Transverse deflections of the interface at $x^* = 0.5$ for a 0°/90° plate for the free vibration problem.

deflections results in the magnitude of the deflection at the bottom surface being significantly larger than the deflection at the top surface. The rate at which these magnitudes are changing decreases as time increases. The small oscillations superimposed on the general sinusoidal response result from wave interactions with the plate boundaries and the interfaces. The initiation and growth of delamination may be observed from Fig. 9, where the jump in displacement across the interfaces evolves as the simulation progresses.

Finally, consider a ramping load, which is applied for 1 μs and subsequently held at the maximum load for 4 μs. The laminate lay-up is (90°/0°/90°/0°/90°) where each of the lamina has an equal thickness. The interfacial stiffnesses (R_n^* and R_s^*) are assumed to be 1.0 for all of the interfaces between the 90° and 0° lamina. Results are presented for the situations where each lamina is modeled using two computational layers. It is noted that higher levels of discretization predict behavior which does not significantly deviate from the case where each lamina is modeled using two computational layers. Using one layer per lamina results in relatively minor deviations.

The macroscopic transverse deflection (u_z^*) for the top surface of the lamina at $x^* = 0.5$ as a function of time is provided in Fig. 10. It is interesting to note that the deflection at the top of the laminate exhibits an oscillatory behavior about a mean response. These oscillations are due to wave reflections from the delaminated interfaces and the boundaries of the plate. The delaminations act as changes in the impedance of the material. This impedance change results in waves being reflected from the interface. Oscillations are not observed in the perfectly bonded case, which is not provided, until the waves reflected from

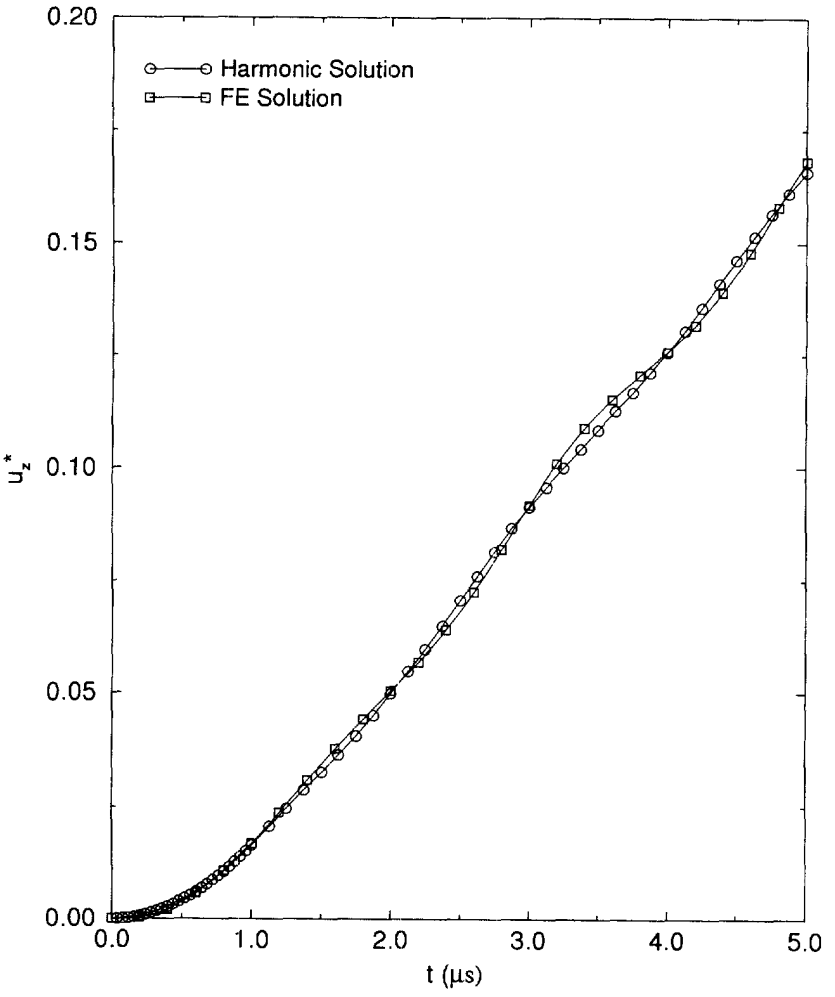

Fig. 10. Transverse deflections at $x^* = 0.5$ for 90°/0°/90°/0°/90° plate for dynamic conditions.

the bottom surface of the plate reach the top surface. The period of these oscillations is much longer for the middle surface than for the top surface. Comparison of the FE solution predictions with the HS results indicates that the overall trends predicted by both solution schemes are in reasonable agreement. However, a phase shift is present between the oscillations predicted by the two solution approaches. Additionally, the magnitude of the oscillations predicted by the FE model are larger than the HS predictions. These differences are a result of the implementation of the Mean Value Theorem in the FE approach for the calculation of the spatial gradients. The averaging affects the strains within the lamina. This results in a faster wave propagation speed for the FE model than for the HS where the averaging is not used. This change in the wave speed results in the phase shift because the reflected waves reach the top surface faster for the FE predictions. An estimate of the wave speed in the transverse direction using $c_T = \sqrt{C_{22}/\rho}$ indicates that the approximate time for a reflected wave from the first interface to reach the top surface is given by $2h_k/c_T$. This estimation closely approximates the predictions given by the HS. It is noted that as the interfacial stiffnesses (R_n^* and R_s^*) increase the oscillations increase. This latter result is not provided in the figure.

Next, the distribution of the transverse (u_z^*) deflection through the thickness of the laminate as a function of time (Fig. 11) is considered. Consistent with expectations, the depth of the wave and, therefore, the displacement magnitudes increase as the time increases. In particular, the rough approximation of the transverse wave speed is in good agreement with the predicted evolution of the depth of the response. Examination of the distributions

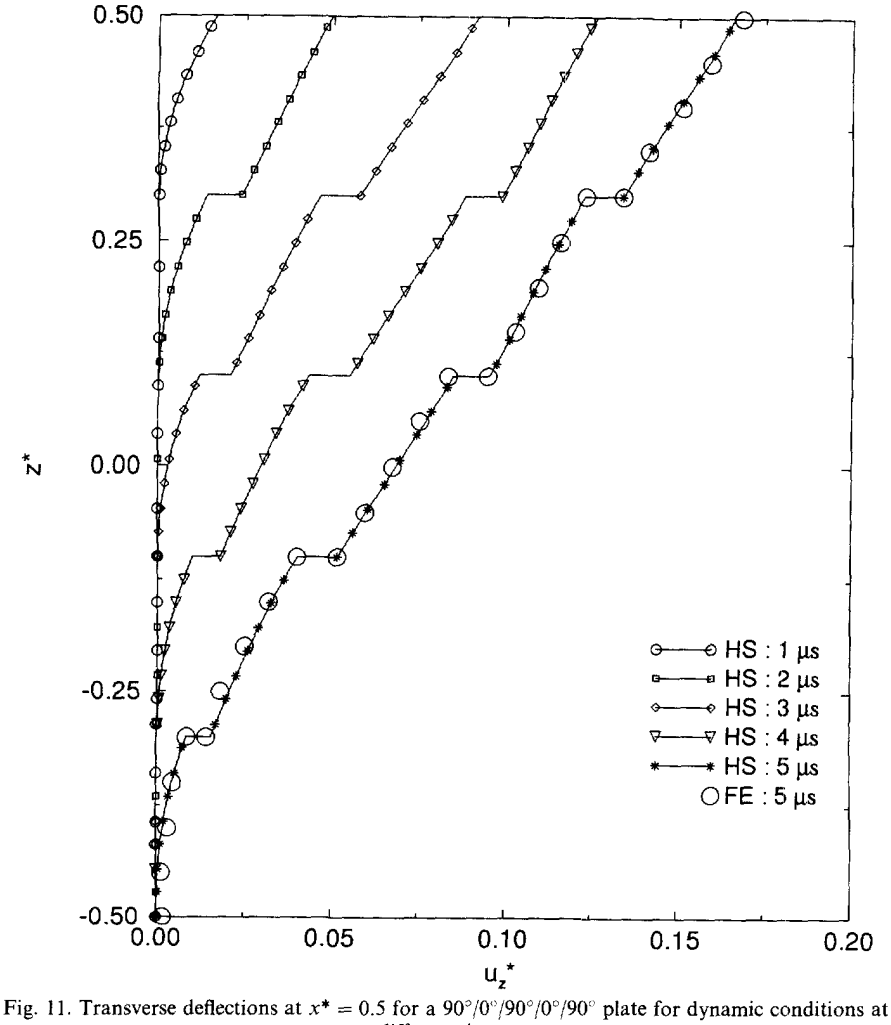

Fig. 11. Transverse deflections at $x^* = 0.5$ for a 90°/0°/90°/0°/90° plate for dynamic conditions at different times.

in the lamina indicates that the evolution of the magnitudes of the displacement is fluctuating as a function of time. Therefore, the slopes of the distributions change as a function of time, which implies that the strain and stress fields do not evolve in a linear fashion. This fluctuation of the slopes in the distributions results from wave reflections. The fluctuation in the fields has a strong effect on the stresses. The displacement jumps at the interfaces also exhibit a nonlinear evolution as a function of time. This fluctuation amounts to changes of about 25% in the magnitude of the jump at the first interface between 2 and 5 μs. It is noted that the relative magnitudes of the jumps for the three interior interfaces is very similar, which indicates that the transverse stresses at these locations are similar in magnitude. As observed in the previous cases, the displacement jumps at the different interfaces constitute about 20% of the overall change in displacement at 5 μs. For comparison, the FE predictions at 5 μs also are plotted on this figure. It can be seen that the agreement is excellent.

The through the thickness distributions of the axial displacement (u_x^*) as a function of time are given in Fig. 12. As observed in the previous cases, the top part of the laminate supports most of the dynamic loading. The extreme values in the distribution occur at the top surface, where the largest negative value is observed, and at the second interface from the top, where the maximum value is observed. At locations below the midplane the distribution rapidly decays and approaches zero at the bottom surface. Under the applied load, the top surface of the plates moves inward while the midplane extends. This response is consistent with the imposed boundary conditions. As time increases the locations of the

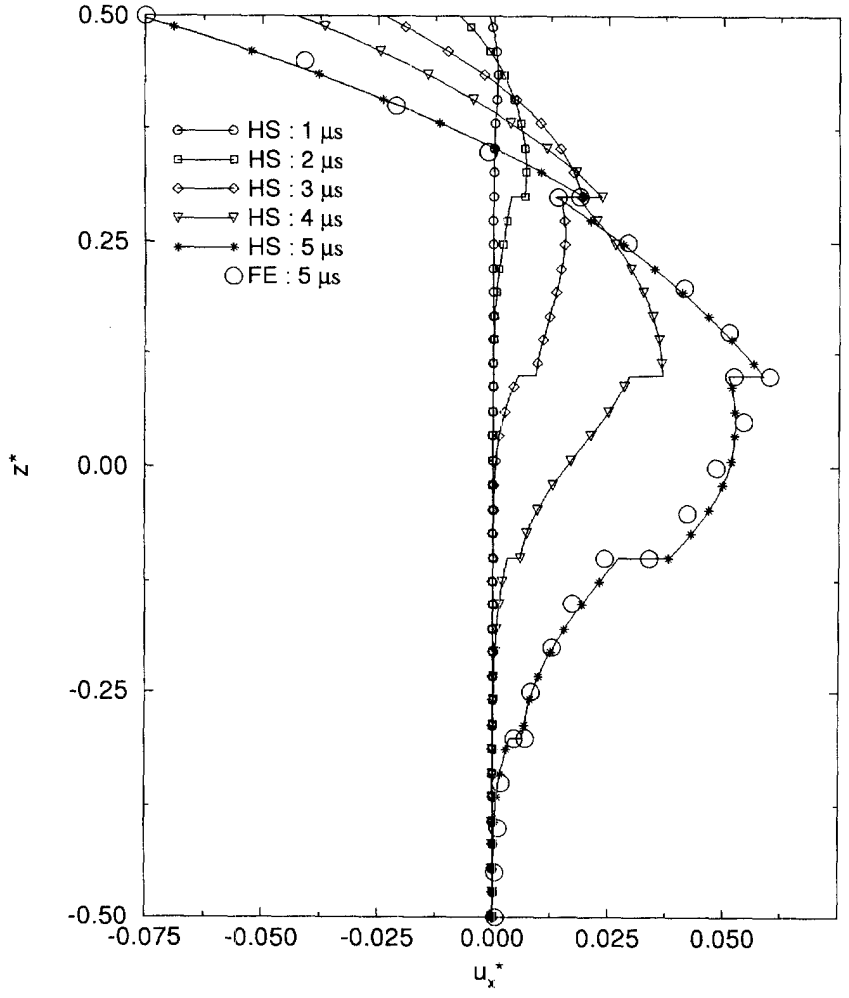

Fig. 12. Axial displacements at $x^* = 0.0$ for a 90°/0°/90°/0°/90° plate for dynamic conditions at different times.

extreme values remain unchanged, while the magnitudes of the displacements at these locations continue to grow. Also, at later times the dynamic effects propagate further into the laminate and therefore more deformation is observed in the lamina closer to the bottom surface. It is important to note that a reversal in the direction of the evolution of the deformation field in the region around the first interface from the top surface occurs, i.e., the axial acceleration is initially positive through the first 4 μs but is negative by 5 μs. Consideration of the slopes of the field within the different lamina indicates that both the magnitude and sign of these slopes change as a function of time. This results in nonlinear distributions for the displacements and rapid variation in the lamina stress field. Consideration of the displacement jumps at the interfaces shows that significant variation in the magnitudes of these jumps is present from interface to interface. At 5 μs, the maximum relative difference is about 333%. This difference in the displacement jumps is caused by the significant variation of the transverse shear stresses. These stresses are greatest in the inner lamina and decay to zero at the outer surfaces of the plate. Fluctuations in the magnitudes of these jumps as a function of time, similar to those observed in the transverse displacement distribution, can be observed. It is noted that as time increases the relative magnitudes of the displacement jumps at the interfaces is largest at locations interior to the laminate. This indicates that the shear stress propagates into the laminate with increasing magnitude as time increases. The initiation and growth of delamination may be observed from Figs 11 and 12, where the jump in displacement across the interfaces evolves as the simulation progresses.

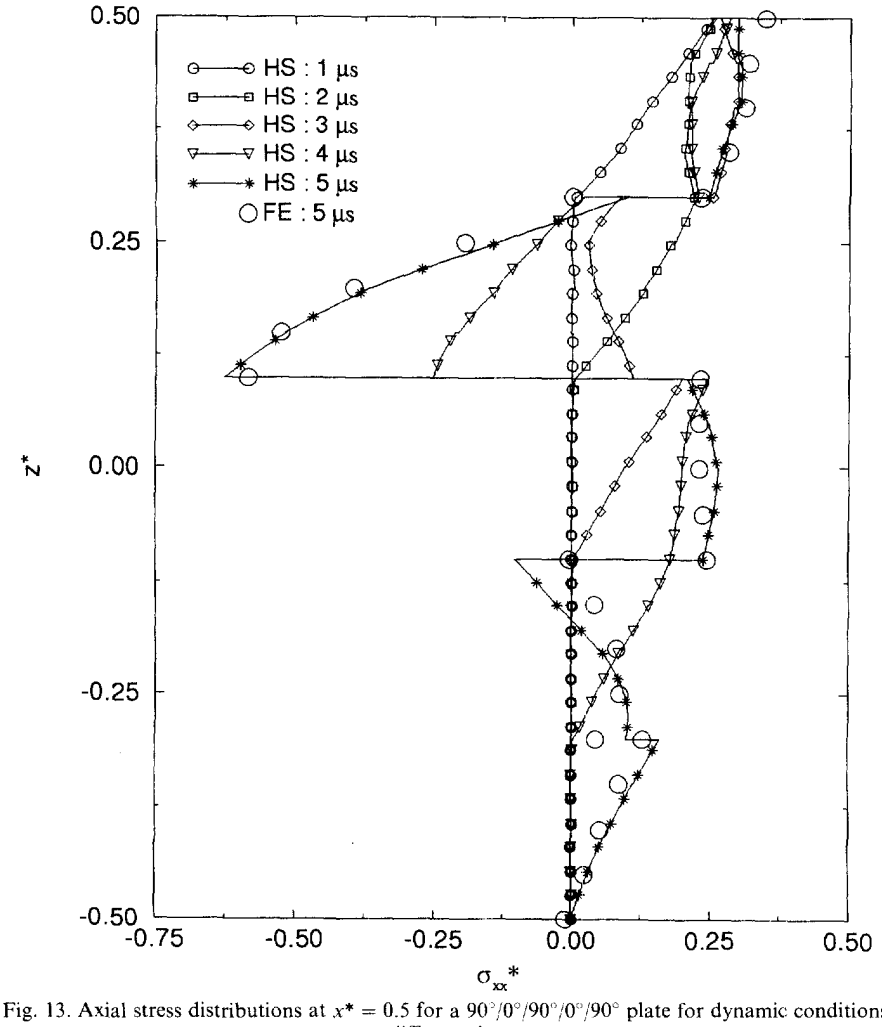

Fig. 13. Axial stress distributions at $x^* = 0.5$ for a 90°/0°/90°/0°/90° plate for dynamic conditions at different times.

The axial stress distribution (σ^*_{xx}) as a function of time at $x^* = 0.5$ is presented in Fig. 13. It can be seen that the stress distribution changes rapidly and in a nonlinear fashion as a function of time and spatial location within the laminate. First the behavior in both of the 0° lamina is considered. In the upper 0° lamina, the axial stress grows in an initially tensile fashion. However, between 2 and 3 μs the magnitude of the stress decreases and by 4 μs the stress is almost fully compressive. Another reversal occurs between 4 and 5 μs causing the top eighth of the lamina to be in tension and the rest to be in compression. Similar trends are present in the lower 0° lamina although the effects occur at much later times and the distributions are reversed. Consideration of the responses of the three 90° lamina shows that in all cases the current loading situation results in purely tensile axial stress distributions. This is an important observation because these types of stresses could result in transverse cracking in the lamina due to the generally low transverse tensile strength of Gr/Ep composites. While oscillations from tension to compression to tension were observed in the 0° lamina, the top 90° lamina exhibits oscillations in the axial stress magnitudes which are purely tensile. In particular, for the first 3 μs the axial stress in this lamina grows increasingly tensile. Between 3 and 4 μs the magnitude decreases but remains tensile. Between 4 and 5 μs the magnitude again grows.

Results for the FE predictions also are provided for the axial displacement (Fig. 12) and stress field (Fig. 13). Good agreement is shown for the HS and FE predictions for the axial displacements. Relatively minor variations of approximately 8% may be observed for the jumps in the interfacial displacement. Larger variations in the comparison of the

axial stress field were obtained. The differences between the two simulations again can be attributed to the method of calculating spatial gradients for the HS and FE formulations.

5. CONCLUSIONS AND SUMMARY

A dynamic, higher-order theory for laminated plates based on a discrete layer analysis has been presented. The formulation includes the effects of delaminations between the layers of the plate. The model implements a generalized displacement formulation at the lamina level. The governing equations for the lamina are derived using variational principles. The equations governing the behavior of the laminate are developed by coupling the layer equations through both the interfacial traction continuity conditions and the interfacial displacement jump conditions. The fundamental variables in the governing equations are the velocities in each layer (v_i) and the interfacial tractions (τ_i).

The theory is not limited to the analysis of thick or thin laminated plates. The approach developed in this paper is applicable to large deformations. However, the numerical implementation of the theory is limited to small deformations because of the assumption that model parameters in the current configuration can be obtained at the locations in the undeformed configuration. It is felt that this is a reasonable assumption for graphite reinforced composites, which fracture at relatively small strains. Furthermore, the cylindrical bending problem used to validate the model was only carried out to small strains. The generalization of the numerical implementation for large deformations would require updating the model parameters on the current configuration. Therefore, a large deformation formation of the plate theory is a straight-forward extension.

The jumps in the interfacial velocities are expressed in an internally consistent fashion as functions of the interfacial tractions. The use of the interfacial tractions as fundamental unknowns is important in predicting delamination behavior in an internally consistent fashion. The formulation has been carried out in a sufficiently general fashion that any constitutive model for the delamination behavior at the interfaces may be incorporated into the theory. No restrictions on the size, location, distributions, or direction of growth of the delaminations have been imposed in the theory. It was demonstrated that the current theory can predict the initiation and growth of delaminations at any interface as well as any interactive effects between delaminations at different locations within the structure. Also, the effects of delamination have been included without restrictions on the constitutive description for the lamina.

It is noted that the computational layers on which the analysis is based can consist of subregions of a lamina, an entire lamina, or several lamina. The ability to incorporate several lamina into a layer would be beneficial in situations where homogenization of a repeated stacking sequence can be used. Furthermore, any general constitutive model may be used to model the response of the lamina.

The generalized plate theory was used to consider the effects of delamination on composite structures under the conditions of dynamic loading. Solutions to the generalized plate theory were obtained both in terms of an harmonic formulation and a general finite-element formulation. Simulations were provided using a linear anisotropic constitutive model for the layers and a linear interfacial constitutive model. Elastic properties for a graphite fiber-reinforced, epoxy matrix composite layers were used in the simulations. Small aspect-ratio (thick) plates were considered in the analyses. Thick geometries provide a challenge for plate theories because of the large through thickness variations in the stress and strain fields. The harmonic formulation was used to validate the theory by comparisons with closed form solutions for a cylindrical bending problem in the quasi-static limit. Excellent agreement was obtained between the harmonic plate solution and the exact cylindrical bending results. The harmonic formulation also was used to investigate the resolution necessary to generate accurate results. Typically, converged results were obtained using two computational layers per lamina. In general, it was found that only one computational layer per lamina provided a sufficiently accurate analysis. Consequently, accurate results can be obtained in an economical fashion.

The harmonic solution was used as a partial validation of the FE formulation for dynamically loaded plates. In general, the comparisons between the harmonic and FE solutions were excellent with differences of approximately 8% between the results. Discrepancies observed between the harmonic and FE results could be attributed to the different techniques used to generate spatial gradients. For the harmonic formulation, local spatial gradients were obtained using the series representation for the velocity fields. However, the FE formulation relied on the Mean Value Theorem to generate spatial gradients, which resulted in a nonlocal description. This resulted in differences in the wave propagation speeds and a subsequent phase shift in the predicted responses.

In the cases considered, delamination was shown to have a significant influence on the displacement and stress fields within the plate. Comparison of simulations, modeling both perfectly bonded and delamination responses, resulted in significant differences in the vicinity of the inter-ply regions. It was shown that the displacement fields for perfectly bonded conditions could not be expected to bisect the displacement distributions, which were obtained when delamination was modeled. The results for both the perfectly bonded and delamination responses converged at locations removed from the interfacial regions.

The dynamic simulations displayed the influence of wave interaction phenomena. Wave propagation through the layers and reflections from the interfacial regions can result in large oscillations of the stress and strain fields through the thickness of the structure. Large stress reversals as well as large differences in the stress fields across the interfacial regions were observed. These effects could exacerbate the potential for damage in layered materials.

Acknowledgements—The authors acknowledge the support of the joint Department of Energy/Department of Defense Munitions Technology Development program. We also would like to acknowledge Dr Mike Stout and Dr Cheng Liu of the Los Alamos National Laboratory for the use of the micrograph provided in Fig. 1. Discussions with Dr John Dukowicz of Los Alamos also are appreciated.

REFERENCES

Aboudi, J. (1991) *Mechanics of Composite Materials: A Unified Micromechanical Approach*. Elsevier, New York.

Barbero, E. J. and Reddy, J. N. (1991) Modeling of delamination in composite laminates using a layer-wise plate theory. *International Journal of Solids and Structures* **28,** 373.

Bolotin, V. V. (1996) Delaminations in composite structures: its origin, buckling, growth, and stability. *Composites: Part B* **27B,** 129–145.

Chattopadhyay, A. and Gu, H. (1994) New higher order plate theory in modeling delamination buckling of composite laminates. *AIAA Journal* **32,** 1709.

Chen, H. P., Tracy, J. J. and Nonato, R. (1995) Vibration analysis of delaminated composite laminates in prebuckled states based on a new constrained model. *Journal of Composite Material* **29,** 229.

Corigliano, A. (1993) Formulation, identification, and use of interface models in the numerical analysis of composite delaminations. *International Journal of Solids and Structures* **30,** 2279.

Finn, S. R. and Springer, G. S. (1993) Delaminations in composite plates under transverse static of impact loads—a model. *Composite Structures* **23,** 177.

Galea, S. C., Shah, L. P. and Sanderson, S. (1995) The effect of multiple damage in composite structures: a theoretical investigation. *Composite Structures* **32,** 383.

Hu, J. S. and Hwu, C. (1995) Free vibration of delaminated composite sandwich beams. *AIAA Journal* **33,** 1911.

Ju, F., Lee, H. P. and Lee, K. H. (1995) Finite element analysis of free vibration of delaminated composite plates. *Composites Engineering* **5,** 195.

Kutlu, Z. and Chang, F. K. (1995) Composite panels containing multiple through-the-width delaminations and subjected to compression. Part I: analysis. *Composite Structures* **31,** 273.

Lo, C. C., Costanzo, F., Zocher, M. A. and Allen, D. H. (1993) Modeling of damage evolution in thick laminates subjected to low velocity impacts. In *Mechanics of Thick Composites*, AMD-Vol. 162, ASME.

Liu, D., Xu, L. and Lu, X. (1994) Stress analysis of imperfect composite laminates with an interlaminar bonding theory. *International Journal of Numerical Methods Engineering* **113,** 570.

McGee, J. and Herakovich, C. T. (1992) Micromechanics of fiber/matrix debonding. Appl. Mech. Prog. Report AM-92-01, University of Virginia.

Narayan, S. H. and Beuth, J. L. (1996) On mode mix designation in composite delamination problems. In *Proceedings of the 14th U.S. Army Symposium on Solid Mechanics*, 16–18 October, Myrtle Beach, SC, U.S.A.

Needleman, A. (1987) A continuum model for void nucleation by inclusion debonding. *Journal of Applied Mechanics* **54,** 525.

Needleman, A. (1990) An analysis of decohesion along an imperfect interface. *International Journal of Fracture* **42,** 21.

Pagano, N. J. (1969) Exact solutions for composite laminates in cylindrical bending. *Journal of Composite Materials* **3,** 398.

Ramkumar, R. L. and Chen, P. C. (1983) Low-velocity impact response of laminated plates. *AIAA Journal* **21,** 1448.

Ramkumar, R. L. and Thakar, Y. R. (1987) Dynamic response of curved laminated plates subjected to low velocity impact. *Journal of Engineering Materials Technology* **109**, 67.

Reddy, J. N. (1987) *Energy and Variational Methods in Applied Mechanics: With an Introduction to the Finite Element Method.* John Wiley and Sons, New York.

Rinderknecht, S. and Kröplin, B., (1995) A finite element model for delamination in composite plates. *Mechanics of Composite Materials and Structures* **2,** 19.

Storakers, B. (1989) Nonlinear aspects of delamination in structural members. In *Theoretical and Applied Mechanics, IUTAM Symposium*, eds P. Germain, M. Piau, and D. Caillerie. Elsevier Science Publishers, Oxford, pp. 315–336.

Sun, C. T. and Qian, W. (1996) The role of friction in the fracture of interfacial cracks. In *Proceedings of the 14th U.S. Army Symposium on Solid Mechanics*, 16–18 October, Myrtle Beach, SC, U.S.A.

Washizu, K. (1968) *Variational Methods in Elasticity and Plasticity*. Pergamon Press, Oxford, England.

Williams, T. O. and Addessio, F. L. (1997) A general theory for laminated plates with delaminations. *International Journal of Solids and Structures* **34**(16), 2003–2024.

Zhen, S. and Sun, C. T. (1995) Modeling multiple delamination in laminated plates. In *Proceedings of ASC*, 10th Technical Conference, 18–20 October, Santa Monica, CA, U.S.A., pp. 483.